

AD-A067 965

CAMBRIDGE UNIV (ENGLAND) DEPT OF ENGINEERING
FRACTURE MECHANISMS IN FIBROUS COMPOSITES. (U)
JAN 79 P W BEAUMONT

F/G 11/4

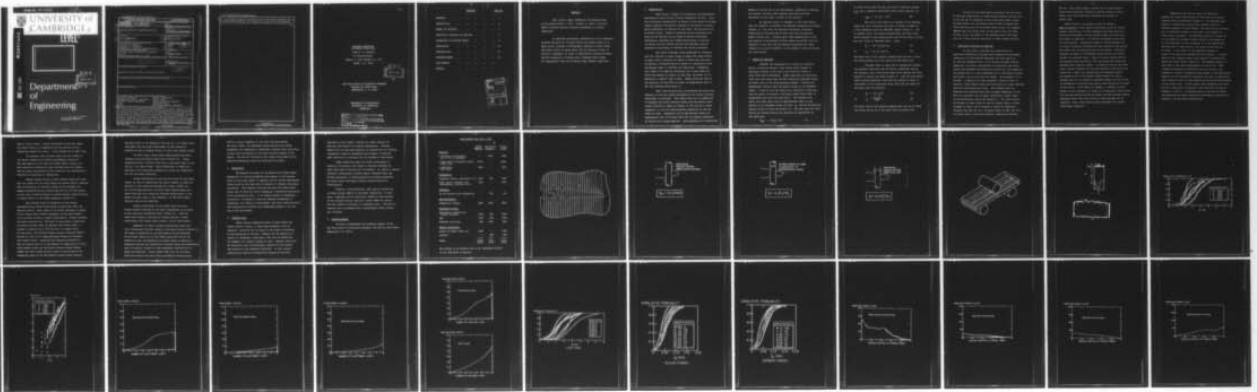
UNCLASSIFIED

AFOSR-TR-79-0489

AFOSR-78-3644

NL

| OF |
AD
A067985



END
DATE
FILMED
6 -79
DDC

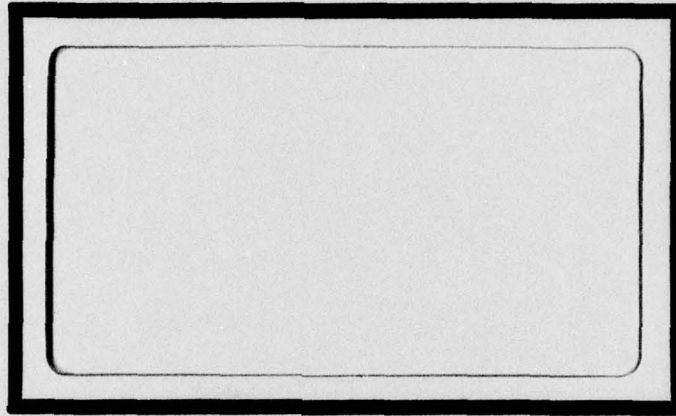
(2) sc



UNIVERSITY of CAMBRIDGE

LEVEL

AD A 067965



DDC FILE COPY

DDC
APR 27 1979
A

Department of Engineering

Approved for public release;
distribution unlimited.

79 04 26 440

19 REPORT DOCUMENTATION PAGE		READ INSTRUCTIONS BEFORE COMPLETING FORM	
1. REPORT NUMBER	2. GOVT ACCESSION NO.	3. RECIPIENT'S CATALOG NUMBER	
18 AFOSR-TR-79-0489		9	
4. TITLE (and Subtitle)		5. TYPE OF REPORT & PERIOD COVERED	
6 FRACTURE MECHANISMS IN FIBROUS COMPOSITES		INTERIM rept. 1 Aug 78 - 31 Jan 79	
7. AUTHOR(s)		8. CONTRACT OR GRANT NUMBER(s)	
10 PETER W. R. BEAUMONT		15 AFOSR-78-3644 ^{new}	
9. PERFORMING ORGANIZATION NAME AND ADDRESS		10. PROGRAM ELEMENT, PROJECT, TASK AREA & WORK UNIT NUMBERS	
UNIVERSITY OF CAMBRIDGE DEPARTMENT OF ENGINEERING TRUMPINGTON ST, CAMBRIDGE ENGLAND CB2 1PZ		16 2307B2 17 B2 61102F	
11. CONTROLLING OFFICE NAME AND ADDRESS		12. REPORT DATE	
AIR FORCE OFFICE OF SCIENTIFIC RESEARCH/NA BLDG 410 BOLLING AIR FORCE BASE, D C 20332		1979	
14. MONITORING AGENCY NAME & ADDRESS (if different from Controlling Office)		13. NUMBER OF PAGES	
11 31 Jan 79		38	
		15. SECURITY CLASS. (of this report)	
		UNCLASSIFIED	
		15a. DECLASSIFICATION/DOWNGRADING SCHEDULE	
16. DISTRIBUTION STATEMENT (of this Report)			
Approved for public release; distribution unlimited.			
17. DISTRIBUTION STATEMENT (of the abstract entered in Block 20, if different from Report)			
18. SUPPLEMENTARY NOTES			
19. KEY WORDS (Continue on reverse side if necessary and identify by block number)			
COMPOSITE, COMPOSITES FAILURE, FAILURE MODE ENVIRONMENTAL EFFECTS, ENVIRONMENT DEBOND, PULLOUT FRACTURE, FRACTURE MECHANISMS ENERGY DISSIPATION MECHANISMS FIBER EXPERIMENTAL DATA MODEL STATISTICAL ANALYSIS, STATISTICS			
20. ABSTRACT (Continue on reverse side if necessary and identify by block number)			
This interim report summarizes the progress made in the period 1 Aug 78 - 31 Jan 79, under grant AFOSR 78-3644 entitled "Fracture Mechanisms in Fibrous Composites. It describes microscopic observations of the debonding, fracture and pull-out of glass fibers and carbon fibers in an epoxy resin; includes a fractographic analysis of glass fibers and carbon fibers in epoxy resin; and an analysis of work of fracture (toughness) in terms of fiber-matrix sliding processes and the dissipation of energy when a debonded fiber snaps. All experimental data was collected under ambient conditions. The approach has been to use models with experimental values			

→ for those parameters adequately measurable and to make simple assumptions about the unmeasurable parameters. This approach uses the most that a model-based theory has to offer and provides a reasonable description of experimental data. ↗

UNCLASSIFIED

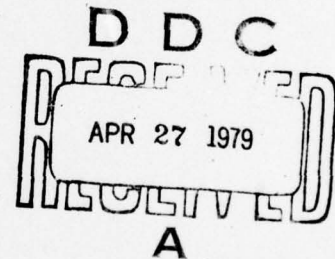
**FRACTURE MECHANISMS
IN FIBROUS COMPOSITES**

Peter W. R. Beaumont

An Interim Report

August 1, 1978 - January 31, 1979

AFOSR - 78 - 3644



**AIR FORCE OFFICE OF SCIENTIFIC RESEARCH
BOLLING AIR FORCE BASE,
WASHINGTON, D. C. 20332**

**DEPARTMENT OF ENGINEERING,
UNIVERSITY OF CAMBRIDGE,
CAMBRIDGE.**

**AIR FORCE OFFICE OF SCIENTIFIC RESEARCH (AFSC)
NOTICE OF TRANSMITTAL TO DDC
This technical report has been reviewed and is
approved for public release IAW AFR 190-12 (7b).
Distribution is unlimited.
A. D. BLOSE
Technical Information Officer**

CONTENTS

PAGE NO.

ABSTRACT	1
INTRODUCTION	2
MODELS OF FRACTURE	3
STATISTICAL ANALYSIS OF FRACTURE	5
ESTIMATION OF FRACTURE ENERGY	8
CONCLUSIONS	12
PROPOSED WORK	12
ACKNOWLEDGEMENT	13
COST BENEFIT	
FIGURES	

ADMISSION for

BY: White Section
 Buff Section

UNANNOUNCED
 JUSTIFICATION

BY: DISTRIBUTION/AVAILABILITY CODES

Dist. Avail. and/or SPECIAL

A

ABSTRACT

This interim report summarises the progress made in the period August 1, 1978 - January 31, 1979, on project FO8671-78-00988 entitled "Fracture mechanisms in fibrous composites".

It describes microscopic observations of the debonding, fracture and pull-out of glass fibres and carbon fibres in an epoxy resin; includes a fractographic analysis of glass fibres and carbon fibres in epoxy resin; and an analysis of work of fracture (toughness) in terms of fibre-matrix sliding processes and the dissipation of energy when a debonded fibre snaps. All experimental data was collected under ambient conditions.

1. INTRODUCTION

There exists a number of alternative, distinguishable mechanisms by which brittle fibrous composites can fail. They are illustrated schematically in Figure 1 which shows an aligned fibrous composite failing by cracking in the matrix, by fibre-matrix debonding, by fracture of the fibre, and by pulling out of broken fibres. Models to describe failure processes like these can be derived and are based on direct microscopic observation; specimens are loaded monotonically to failure in tension and the fracture surface and specimen interior examined by microscopy to identify the failure processes.

The report discusses three mechanisms in connexion with the fracture of glass fibres in epoxy and carbon fibres in epoxy using a sequence of events in which they may occur. An equation is selected which is based on a physically sound microscopic model to describe each mechanism. Frequently, this leads to an equation containing one or more terms for which only bounds are known; in this case, the model is too imprecise to predict exact values. Theory gives the form of the equation; we then have to resort to experimental data to set the constants which enter it.

Next, some fracture data is presented and using each equation in turn the energy dissipated by the various fracture mechanisms is estimated. This energy data will be summarized in diagrams which show fracture energy plotted against fibre volume fraction or number of fibres; in the case of a hybrid composite, it will be plotted against proportion of the two kinds of fibre. Comparison can be made between theory and experimental work of fracture data and the dominant mechanism of failure will become apparent. Each mechanism will undoubtedly

depend in its own way on the environment, temperature, humidity, for example; fracture under ambient conditions has been considered in the first 6 months of the program.

An important point to remember is that when moving from one composite to another, the dominant mechanism of fracture changes; so, too, does the detailed microscopic processes underlying the fracture and we shall see that the physical models confirm this. Another point worth emphasizing is that the sequence of microscopic failure events can differ from one composite to the next and the energies dissipated and their origins can be quite different in the stages of crack initiation and crack growth.

2. MODELS OF FRACTURE

Consider the propagation of a crack in a brittle matrix, around and beyond a long strong fibre (Figure 2). Localised stresses at the tip of the crack are likely to cause fibre-matrix debonding. Under conditions of increasing load, the crack faces open and the interfacial debonded region on either side of the crack surfaces extends. Differential displacement between fibre and matrix occurs in the debonded region. It may be that the fibre still interacts in some way with the matrix to provide a frictional shear force which is established soon after the bond fails. The distance over which this shear force acts is approximately equal to the product of the debonded length of fibre, l_d , and the differential failure strain of fibre and matrix, $\Delta\epsilon$. The work done per fibre during the sliding process can therefore be represented by the expression

$$W_{pdf} = \pi d \tau l_d^2 \Delta\epsilon / 2 \quad (1)$$

In terms of the work done per unit area of fracture surface, γ_{pdf} , for a composite containing fibre volume fraction, V_f :

$$\gamma_{pdf} = V_f \tau l_d^2 \Delta \epsilon / d \quad (2)$$

The load on the fibre is a maximum in the debonded region and as it increases the fibre is likely to break at a flaw somewhere along its debonded length (Figure 3). For an elastic fibre, the energy released when the fibre snaps can be equated to the deformational work of the fibre, $\sigma_f^2 / 2E_f$, per unit volume of debonded fibre. Hence

$$W_d = \pi d^2 \sigma_f^2 l_d / 24 E_f \quad (3)$$

or
$$\gamma_d = V_f \sigma_f^2 l_d / 4 E_f \quad (4)$$

The exact form of the equation depends upon the way in which the stress builds up in the fibre from the broken end.

Provided there is some kind of interaction between the debonded fibre ends and the matrix, mechanical keying, for instance, then a frictional shear force opposes any force applied to extract the fibre (Figure 4). Like the post-debond fibre sliding mechanism, fibre pull-out energy is equal to the product of the frictional shear force and the square of the fibre pull-out distance;

$$W_p = \pi d \tau l_p^2 / 6 \quad (5)$$

or
$$\gamma_p = \frac{V_f \tau l_p^2}{12d} \quad (6)$$

The exact form of the equation depends upon the way in which the stress builds up in the fibre from the broken end.

In each of the three models presented, the work done is directly proportional to fibre volume fraction and each one, in its own way is sensitive to the interfacial shear stress. We might expect the interfacial shear stress to depend upon fibre spacing since the frictional shear stress, for example, depends upon the radial force of the matrix onto the fibre. If this is so, the length of the debonded region and fibre pull-out length would be sensitive to fibre volume fraction.

3. STATISTICAL ANALYSIS OF FRACTURE

At this point I describe the construction of cumulative probability diagrams which summarize fractographic information on fibre-matrix debonding and fibre pull-out. It involves assembling data on the failure of model fibrous composites in tension, determining the distances over which fibres have debonded and fibres have pulled out, and computing the probability of a fibre debonding over a particular distance and having a particular pull-out length. The procedure is as follows. I tabulate for each composite, values of work of fracture, fibre debond length and fibre pull-out length obtained from 20 or more duplicate tests. The fracture data are obtained from flexural beam tests on model composites in the form of a prismatic bar of epoxy containing a single layer of uni-directional fibre tape (Figure 5). The tape consists of rovings of glass fibres or tows of carbon fibres or both, arranged in such a way to produce a series of composites ranging from 100% (by vol.) of glass fibres to 100% (by vol.) of carbon fibres, with many different combinations between

the two. This figure shows a single tow of carbon fibres (with 5,000 individual filaments) and two rovings of glass fibres (with 1600 individual filaments per roving) on either side.

After fracture, an attempt is made to assign a mode of failure to each group of specimens, based on fractographic observations of fibre debonding and fibre pull-out. A precise measurement of fibre debond length and fibre pull-out length is important. An optical microscope can be used for this purpose. Tracings are made of each protruding tow or roving, carefully following the dark outline of the pulled out fibres and the fracture plane of the matrix. Similarly, tracings are made of the debonded regions which are clearly visible in reflected light. Figure 6 shows a broken half of the specimen shown previously with the pulled out fibres and debonded fibre regions visible. A tracing of one of the glass fibre rovings is shown with the dark profile of the pulled out fibres and a light area representing the debonded region. An average value of the longest fibres pulled out and an average value of the length of debonded fibres for each roving is determined by dividing the area of each tracing by the width of the roving. If we have, for example, 5 rovings of glass fibres in each specimen in a group of 20 specimens, then we have 200 tracings showing pulled out fibres and 200 tracings showing debonded fibres since both halves of each specimen can be examined. First, some fracture data collected for a glass fibre-epoxy composite.

Summarizing the data in plots of cumulative probability versus fibre debond or fibre pull-out lengths produces useful information (Figure 7). The diagram shows cumulative probability versus fibre debond length for different numbers of glass fibres. The data does not overlap but is displaced slightly to the right as the number of glass fibres increases. The debonding process is sensitive to the number of rovings of glass fibres in the composite. It is interesting to note (although it is not obvious why) the data for $N = 4800$ falls to the right of the data for $N = 6400$. I will refer to this apparent reversal in trend of the cumulative probability data shortly. A similar shift of data towards higher fibre lengths is observed for pulled out glass fibres (Figure 8). The apparent oddity in this case is the large displacement of data for $N = 8000$. A Weibull expression can describe each set of data, the constants or Weibull parameters which appear in the exponential equation can be obtained by replotting the data in logarithmic form (Figures 9 and 10) and determining the slopes and intercept of the linear plot. In both cases, fibre debonding and fibre pull-out, data falls on parallel lines each with a slope of between 1.5 and 2.5. Presenting data in this way is useful for observing the subtle effects of environment, moisture for instance, and characterising fracture.

4. ESTIMATION OF FRACTURE ENERGY

It is not clear at this stage whether an average value of fibre debond length and fibre pull-out length together with the models of fracture is sufficient to estimate reasonably accurately the work to fracture the composite or whether a more rigorous statistical analysis needs to be developed.

As a first approximation, let us take the average values of glass fibre debond length and pull-out length. The diagram of fracture energy versus number of glass fibres (Figure 11) shows the estimated energy dissipated during the post-debond sliding mechanism. The relationship is not a simple linear one as one would expect from the form of the equation; the cumulative probability data shows fibre debond length to be sensitive to the number of fibres in the composite. We recall that it is the square of the fibre debond length and volume fraction of fibres which appears in the post-debond fibre sliding equation. The plateau to the curve reflects the reversal in the trend of cumulative probability data for $N = 6400$ fibres to which I referred earlier.

An estimation of fibre deformational energy often referred to as fibre debond energy is shown in the next diagram (Figure 12). At first sight, the shape is linear but closer examination shows a smooth curve with a gradually increasing slope. Again, it reflects the dependence of fibre debond length on the number of glass fibres. The plateau shown in the previous figure is less obvious since fibre debond energy is directly proportional to the length of debonded fibres. The energy dissipated in this way is significantly less than the work done in the post-debond fibre sliding mechanism.

The work to pull broken glass fibres out of a cracked matrix is of a similar order of magnitude as the fibre debond energy (Figure 13). Both figures have a similar shape; the increase in gradient of the curve at the high volume fraction originates from the high values of fibre pull-out length shown previously in the cumulative probability data for $N = 8000$.

The result of summing these 3 energy parameters is shown in Figure 14. Apart from a small rise in the curve at $N = 5000$ fibres, approximately, it is a smooth curve with a gradually increasing slope as the number of fibres increases. Comparison of the empirical diagram with experimental work of fracture data shows remarkable likeness in shape and magnitude (Figure 14). From observations of the fracture of glass fibres in epoxy we know that the composite exhibits all the common modes of failure; matrix cracking, fibres debonding, fibres snapping and fibres pulling out. The dominant toughening mechanism appears to be post-debond sliding between fibre and matrix; the breakage of fibres and the pulling out of the broken ends dissipate similar amounts of energy and together contribute little more than one-quarter of the total fracture energy of the composite.

Fractographic information of glass fibres in a hybrid composite of glass fibres and carbon fibres is summarized in the following cumulative probability diagrams (Figures 15 and 16). The fibre debond length data does not superimpose; increasing the ratio of glass fibres to carbon fibres may displace the data to the right or to the left (Figure 15). For example, increasing the glass fibre content from 30% (by vol.) to 56% (by vol.) of the total fibre content shifts the data from low values of fibre debond length to high values of fibre debond length: increasing the glass fibre content a further 7% (by vol.) moves the data

back to lower values. Closer examination of the data shows the subtle effects of composition on the position of the cumulative probability curve. I will remind you of them later.

In contrast, data of glass fibre pull-out length in the hybrid composite are almost superimposed (Figure 16). The same applies to the data for carbon fibres (Figure 17). Each cumulative probability curve overlaps with one another and the shape and position of the curves are not significantly affected by variations in composition.

Taking average values of fibre debond length and fibre pull-out length for the glass fibres and carbon fibres, combined with the equations of fracture energy we can estimate the energy dissipated during fracture and pull-out of both fibres. In this case, fracture energy is plotted against volume fraction of carbon fibres in the hybrid composite (Figure 18).

This diagram shows an estimation of the energy dissipated during glass fibre-matrix sliding soon after the bond has failed. While there is an overall decrease in energy as the carbon fibre content increases, as one would expect, it by no means follows a linear relationship. Certain features are worth pointing out. The first is that after a sharp drop in energy as glass fibre is replaced with carbon fibre, a plateau is observed up to 40% (by vol.) of carbon fibre. At that point, the fracture energy actually increases before falling to zero as the remaining glass fibres are replaced with carbon fibres. Recalling the cumulative probability data we realize that it is the effects of composition on glass fibre debond length and the subtle balance between debond length and fibre volume fraction which is the origin of the unexpected shape of the post-debond sliding energy diagram.

The small peak in the diagram at 44% (by vol.) of carbon fibre coincides with the large displacement of the cumulative probability data to higher values of glass fibre debond length.

At first sight, glass fibre debond energy decreases linearly with increasing carbon fibre (Figure 19). Closer inspection shows a shallow curve with a very small peak at 44% (by vol.) of carbon fibre. Minor differences in shape and position of the cumulative probability curves are responsible for the non-linear behaviour.

Slight undulations in the pull-out curve for the glass fibres can also be identified with minor changes in shape and position of the cumulative probability curves (Figure 20). As a first approximation, the glass fibre debond energy and glass fibre pull-out energy are directly proportional to the amount of glass fibre in the composite, as one would expect from the form of the equations.

Similar undulations in the carbon fibre pull-out energy diagram originate in the small differences to be found in the cumulative probability data (Figure 21). Ignoring these minor effects, the pull-out energy follows a linear relationship with carbon fibre content, as one would expect.

Summation of these 4 energy contributions gives the total theoretical fracture energy of the hybrid system (Figure 22). The shape is dominated by the post-debond sliding mechanism of the glass fibres but at the carbon fibre-rich end of the diagram the pull-out mechanism of carbon fibres is important. Comparison between the theoretical fracture energy and experimental work of fracture (Figure 22) show remarkable similarities in shape and magnitude. These results show that for the glass fibre-rich hybrid the glass fibre post-debond sliding energy

term is a major component of the total fracture energy. For glass fibres, the debonding energy and pull-out energy parameters are comparable in magnitude; together they contribute no more than one-quarter of the total fracture energy of the hybrid. The work of fracture of the carbon fibre-epoxy can be explained adequately using the fibre pull-out model.

5. CONCLUSIONS

The approach has been to use models and to make simple assumptions of certain parameters that appear in the analyses which we have been unable to measure; and to include experimental values which we have been able to measure or estimate reasonably accurately. This approach utilizes the most that model-based theory has to offer but still attempting a reasonable description of the experimental data. It is useful because in designing a structure it is helpful to know the dominant mechanisms of toughening, the effects of environment, and their characteristics. Each mechanism of fracture will undoubtedly depend in its own way on the environment.

6. PROPOSED WORK

Model fibrous composites based on glass fibres and carbon fibres in epoxy, in some cases polyester, will be prepared. Attention will be given to the effect of moisture on the mechanisms of failure. Samples will be exposed to a variety of atmospheric conditions, high and low humidities, for example, for varying lengths of time. Fracture tests will be carried out and a fractographic analysis of the surface and interior of the composite completed. It will involve constructing cumulative probability diagrams of the kind

described in this report, looking for subtle effects of moisture and kinetics of moisture degradation. Fracture models will be used where possible to analyse work of fracture (toughness); material parameters which appear in them and show sensitivity to moisture will be studied in some detail.

Under conditions where the carbon fibre-epoxy is sensitive to moisture, the effect of surface treatment of fibre upon mode of failure will be studied. Dr. David H. Kaelble (Rockwell International Science Center, Thousand Oaks) may provide assistance in characterising the surface properties of carbon fibres and supply surface treated fibres for investigation.

Finally, a few preliminary tests may be carried out to study fatigue effects in the model composites. In this case, a specimen will be cyclically loaded at some fraction of the ultimate failure load for a given number of cycles, and then loaded to fracture in a monotonic test. The work to fracture will be measured and a fractographic study carried out as before.

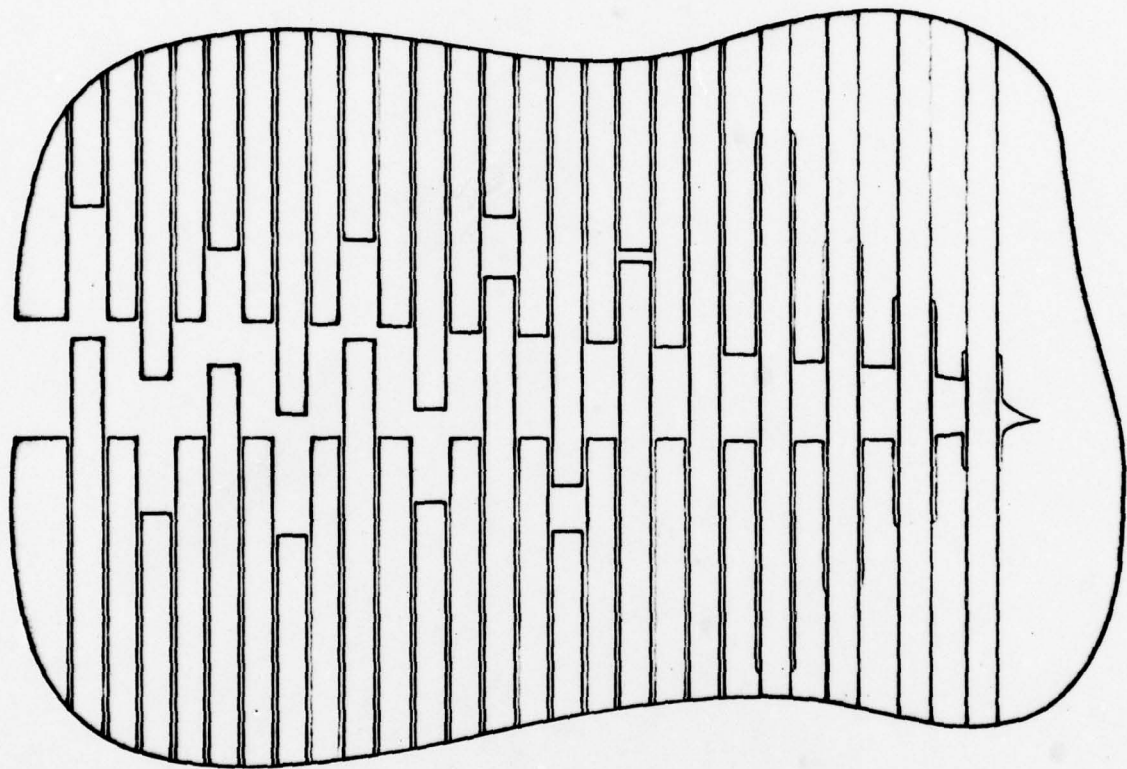
7. ACKNOWLEDGEMENT

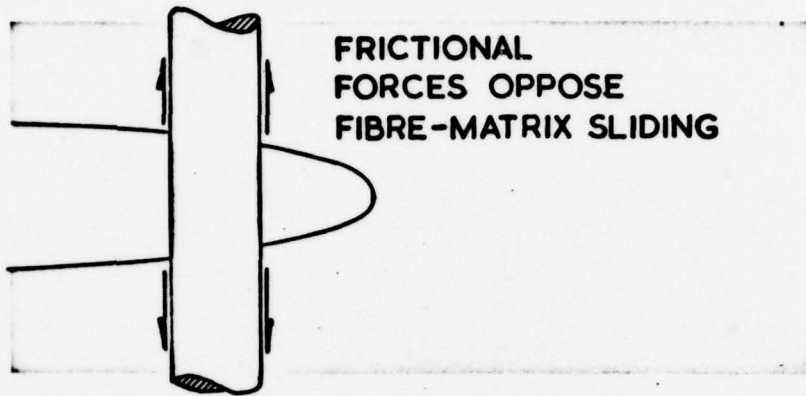
We wish to acknowledge the financial support of the Air Force Office of Scientific Research, Bolling Air Force Base, Washington, D.C. 20332.

COST BENEFIT FOR 1979 - 1980

	\$		
	<u>AFOSR</u> <u>Support</u>	<u>University</u> <u>Support</u>	<u>Project</u> <u>Cost</u>
<u>SALARIES</u>			
1 Principal Investigator (Dr. P. W. R. Beaumont)	-	2200	2200
1 Post-doctoral Research Fellow (100% time)	12100	-	12100
1 Technician (50% time)	3500	-	3500
<u>CONSUMABLES</u>			
Polymers, fibres, stationery, etc.	1800	700	2500
Final report (draught work, photography, printing, etc.)	1500	-	1500
<u>OVERHEADS</u>			
(@ 15% salaries and consumables)	-	435	435
<u>NON-CONSUMABLES</u>			
Temperature chamber	4000	4000	8000
<u>EQUIPMENT CHARGES</u>			
Maintenance expenses for Instrom machines	1500	500	2000
SEM	1700	500	2200
Workshop facilities	600	1200	1800
<u>TRAVEL SUBSISTENCE</u>			
Visits to AFOSR, AFML, etc.	2500	-	2500
Internal	-	400	400
TOTAL	<u>29200</u>	<u>9935</u>	<u>39135</u>

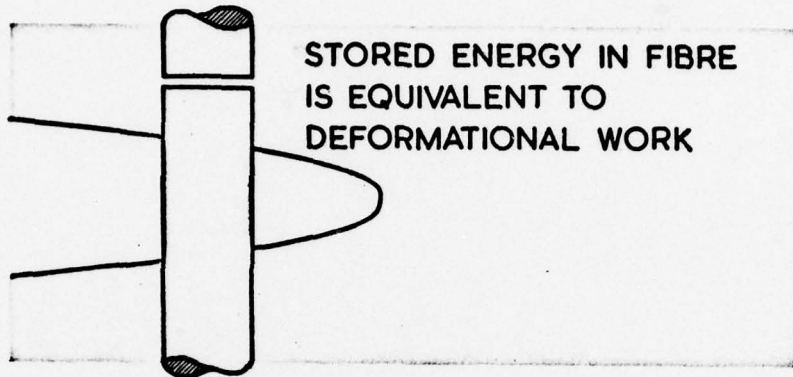
This budget is an estimate and is not considered binding
in the individual categories.



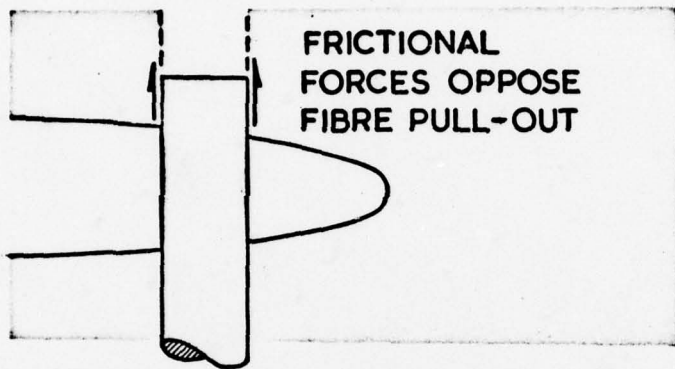


FRICTIONAL
FORCES OPPOSE
FIBRE-MATRIX SLIDING

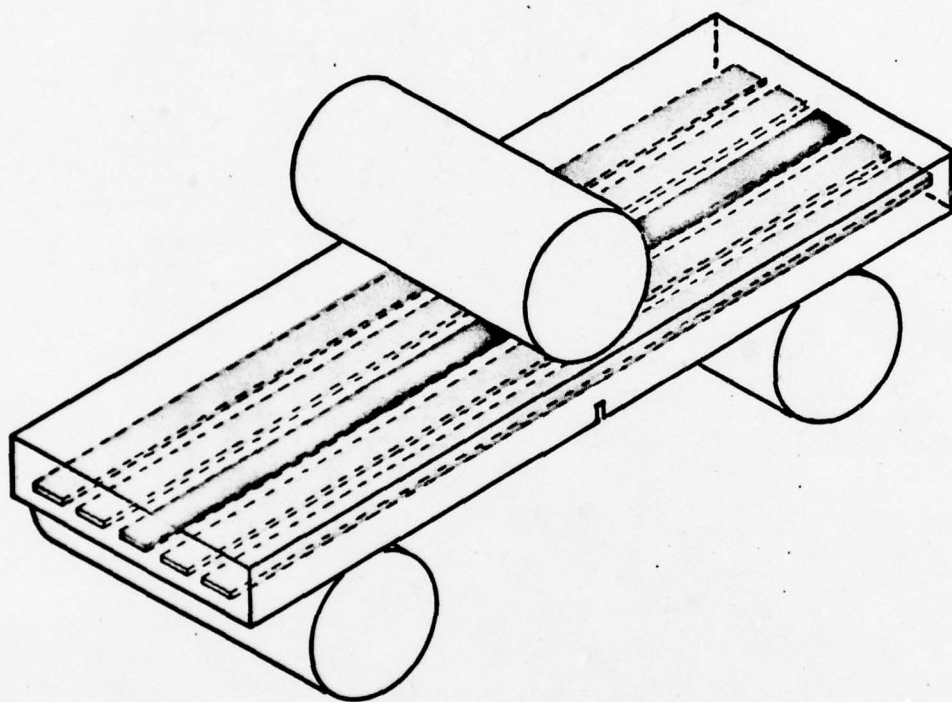
$$\gamma_{pdf} = V_f \tau y^2 \Delta \epsilon / d$$

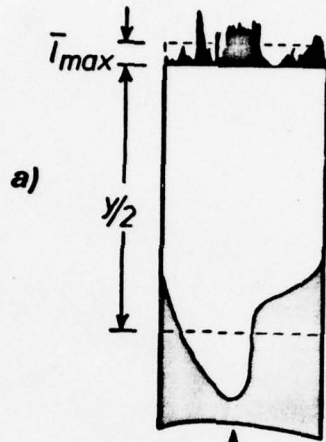


$$\gamma_d = v_f \sigma_f^2 \gamma / 4E_f$$



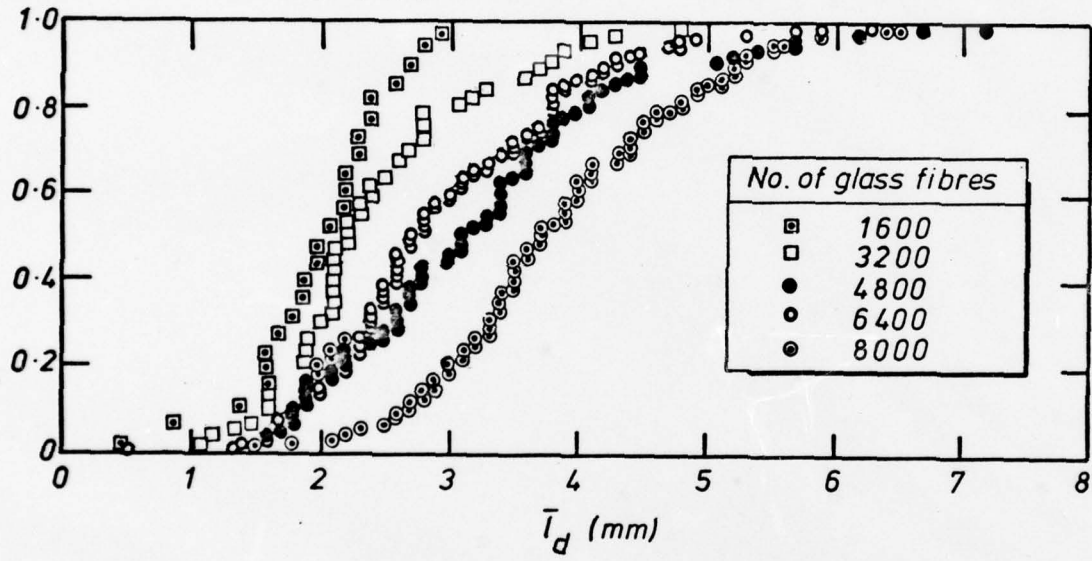
$$\gamma_p = v_f \tau l_c^2 / 12d$$



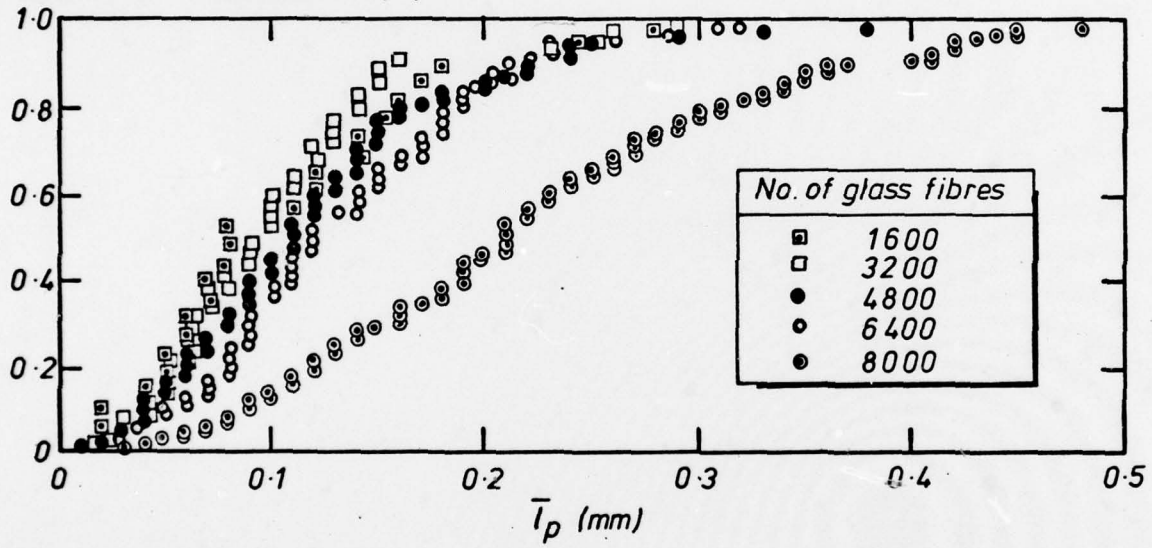


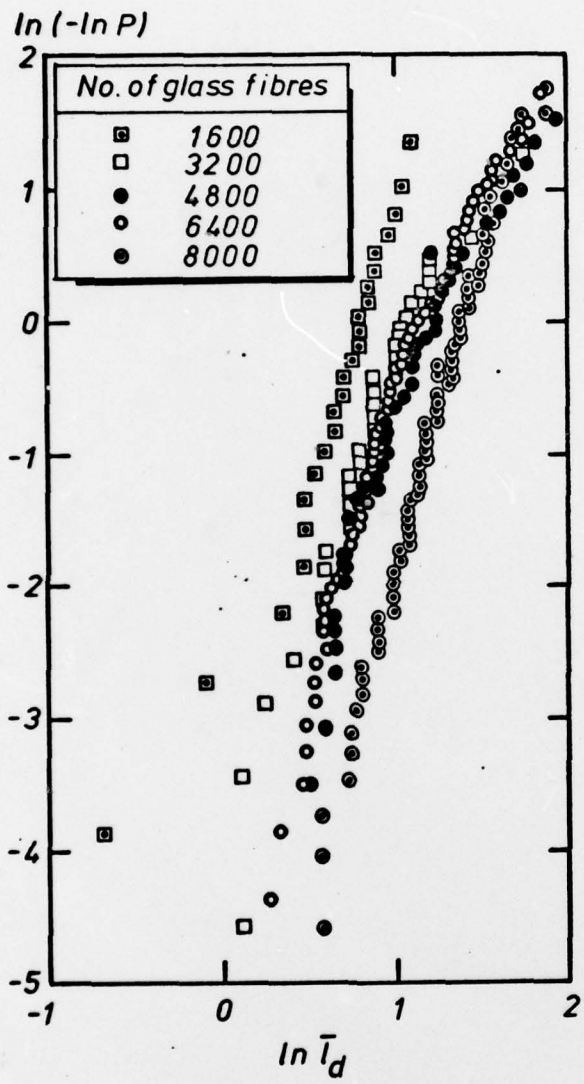
b)

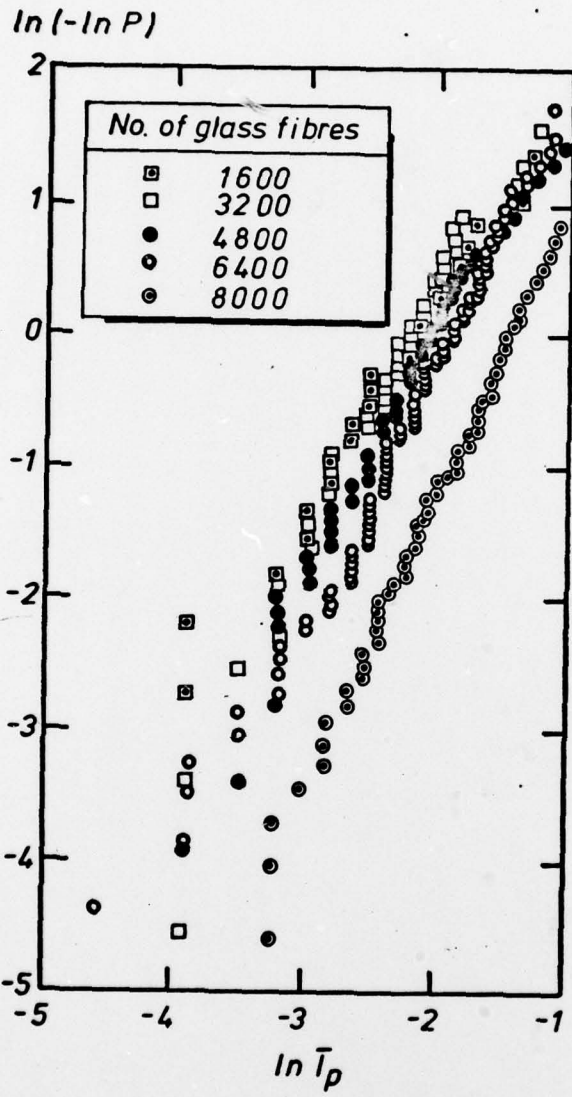
CUMULATIVE PROBABILITY (P)



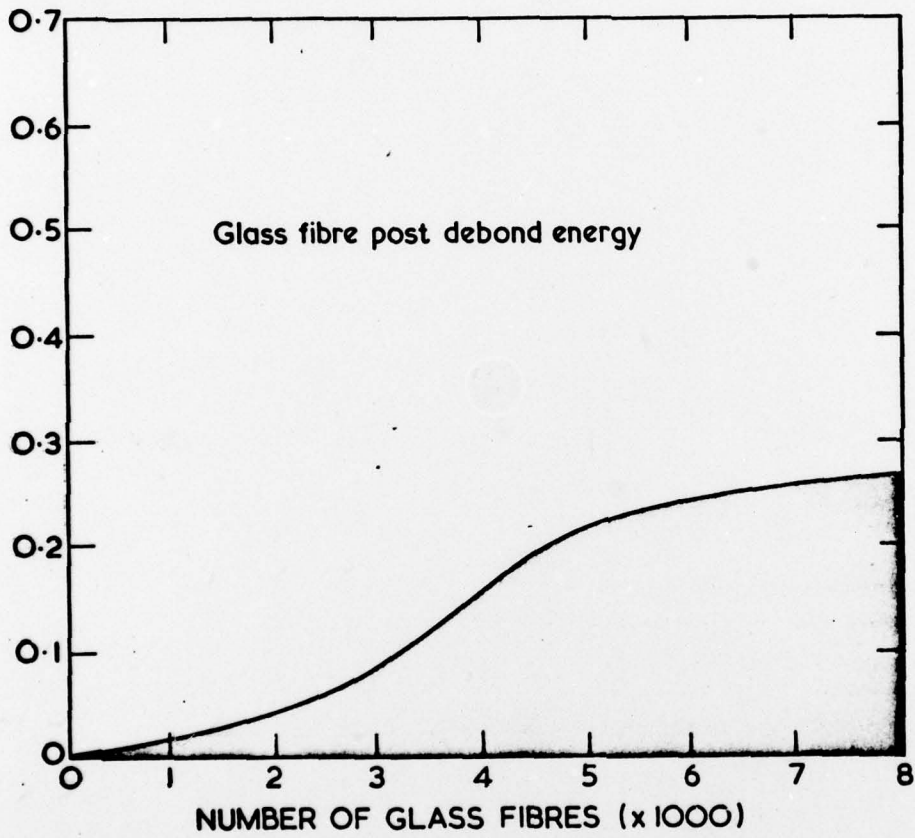
CUMULATIVE PROBABILITY (P)



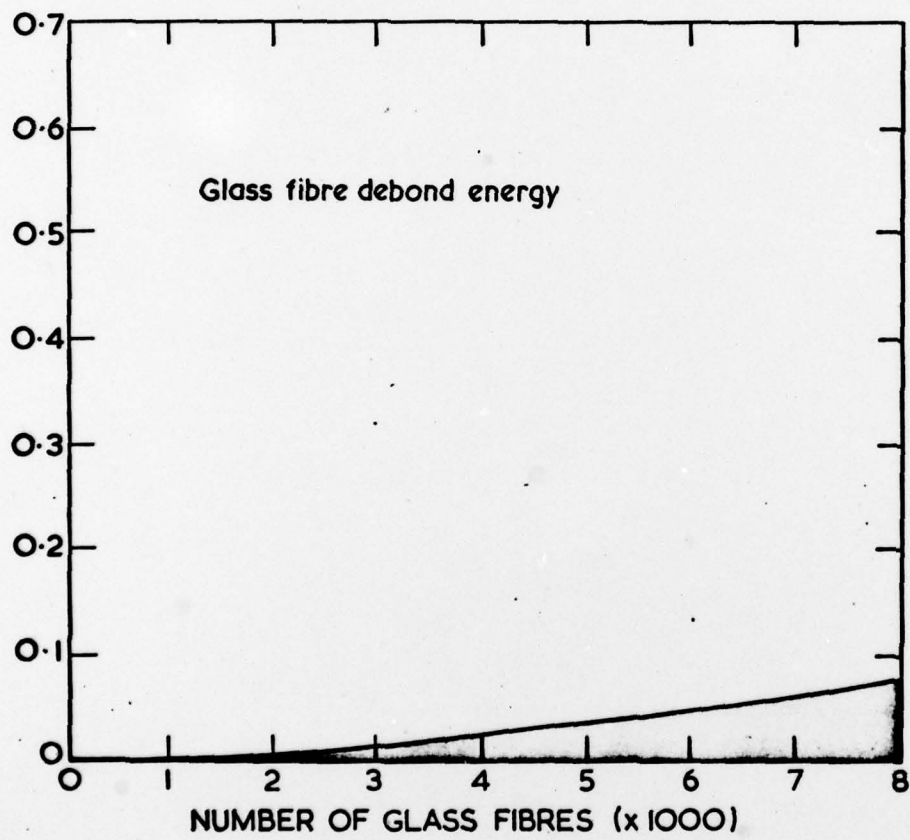




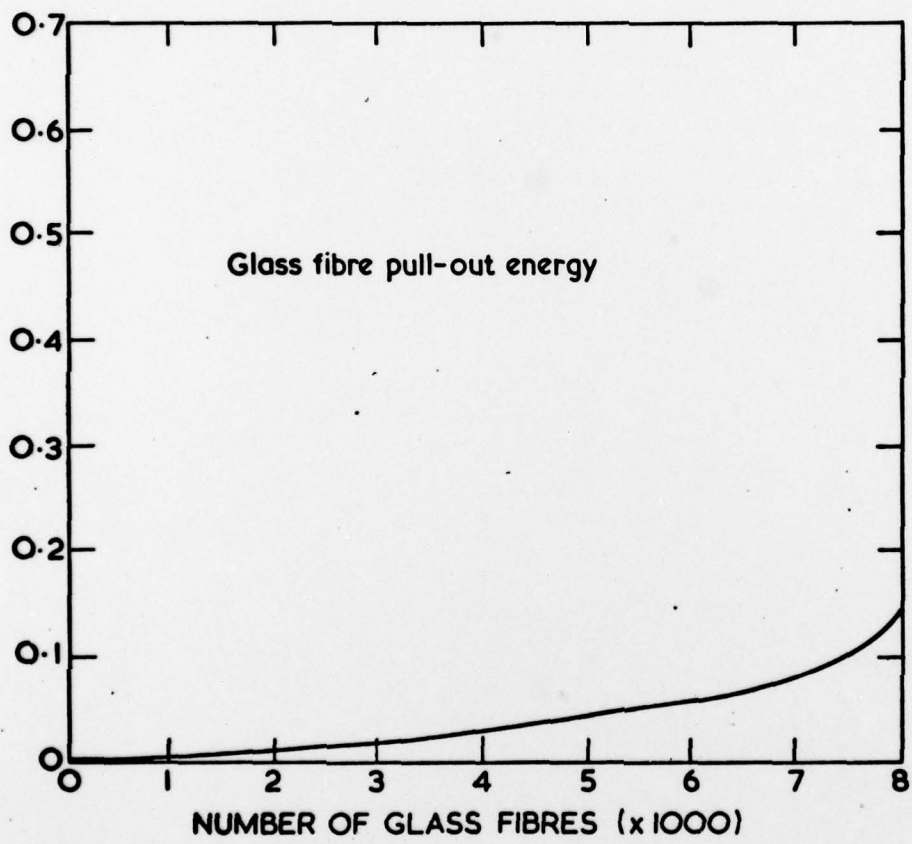
ATURE ENERGY (JOULES)



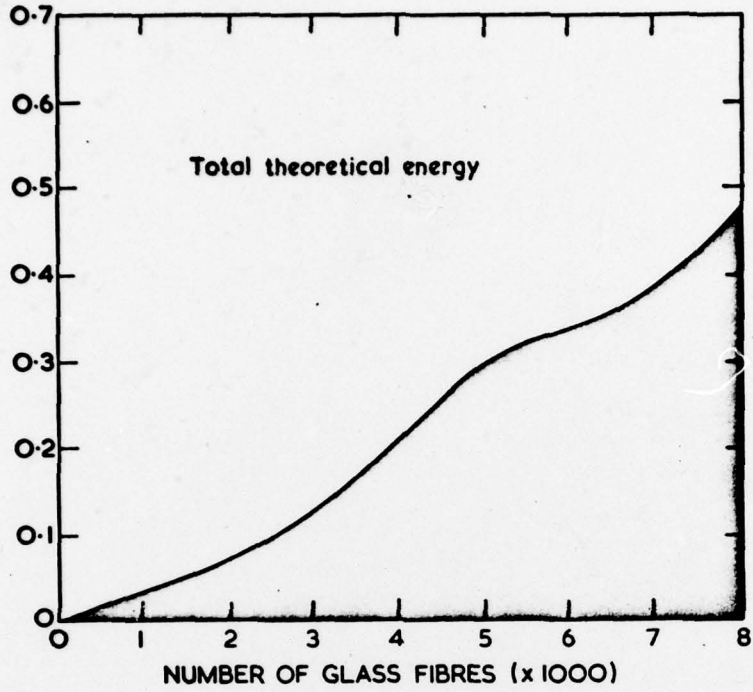
ATURE ENERGY (JOULES)



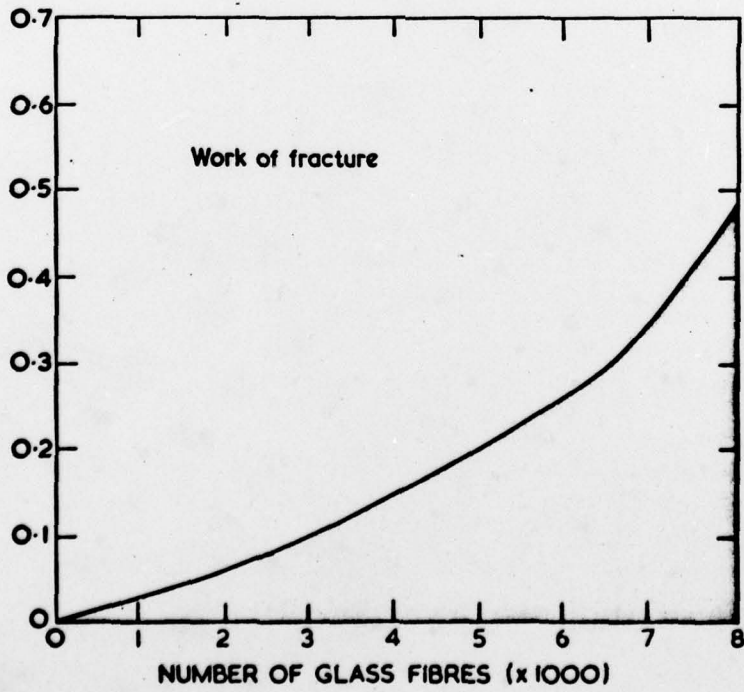
STRUCTURE ENERGY (JOULES)



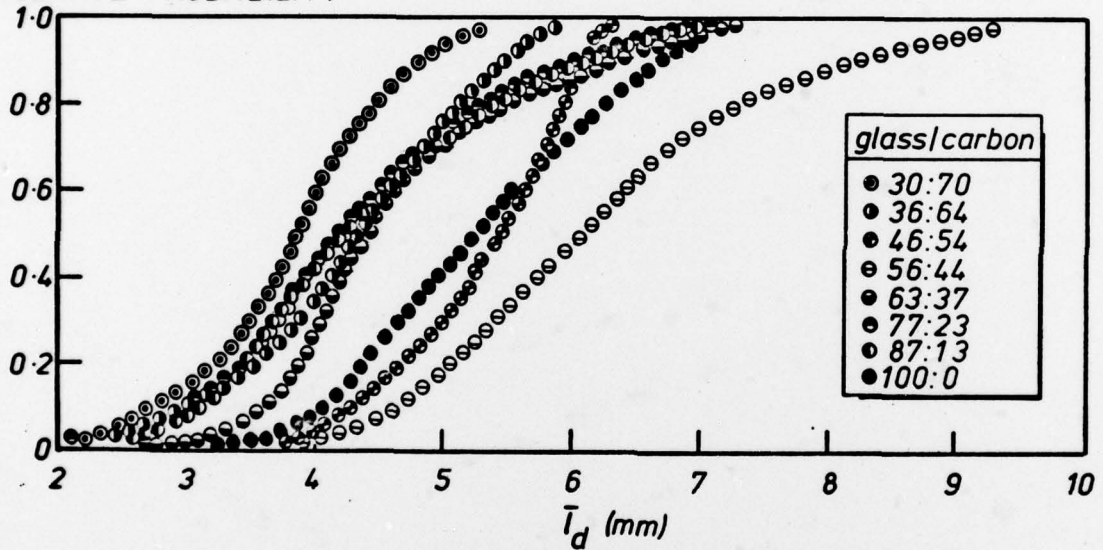
FRACTURE ENERGY (JOULES)



FRACTURE ENERGY (JOULES)

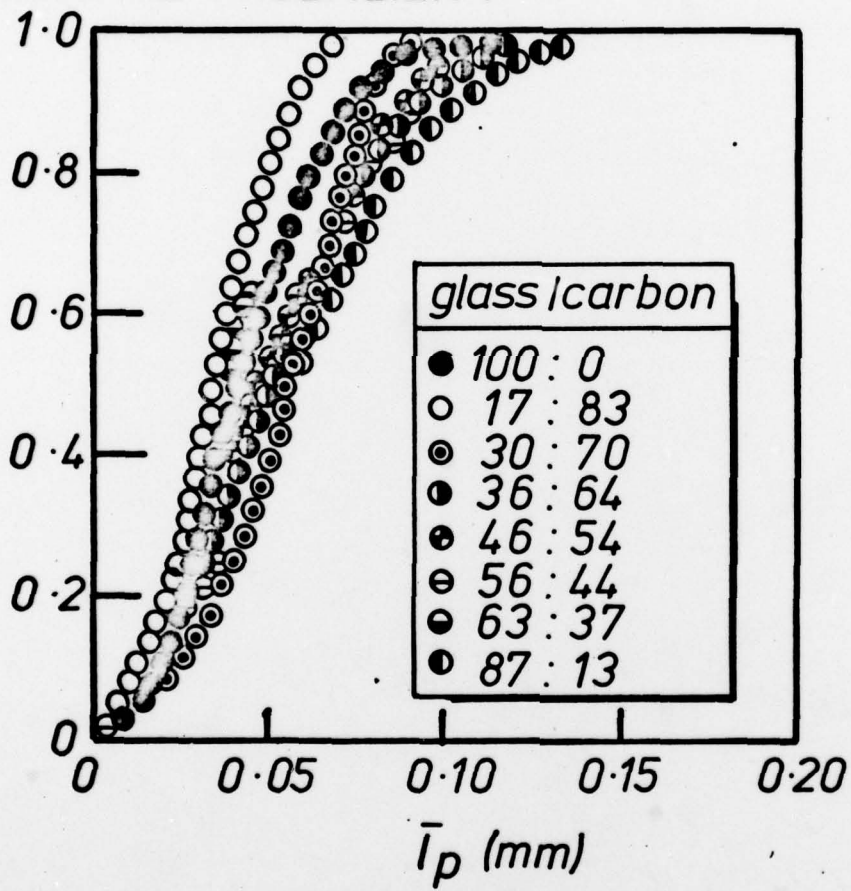


CUMULATIVE PROBABILITY



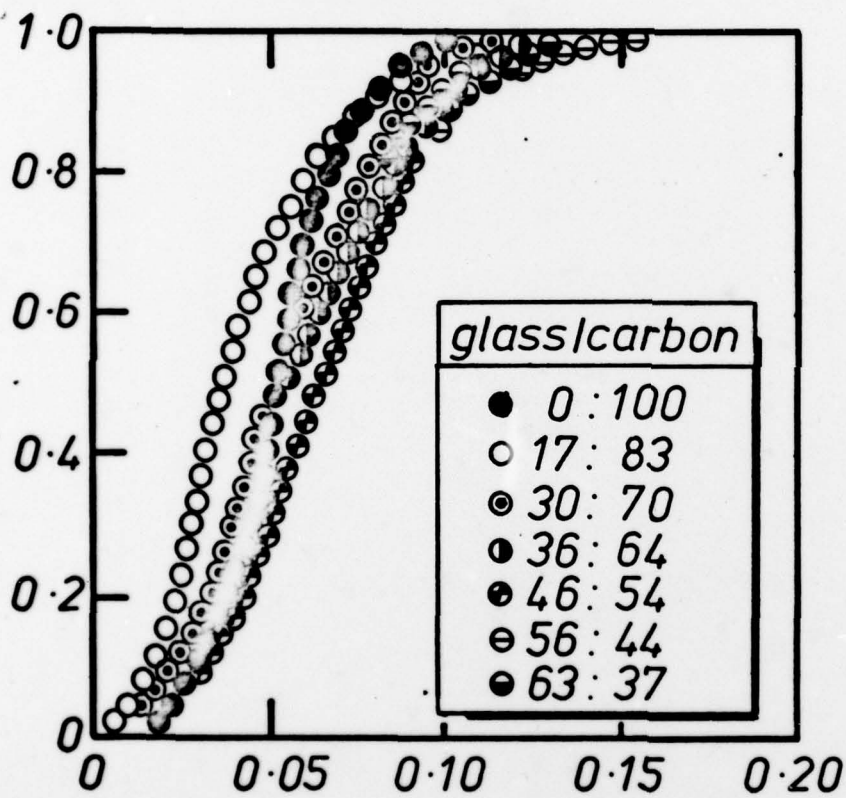
GLASS FIBRES

CUMULATIVE PROBABILITY



GLASS FIBRES

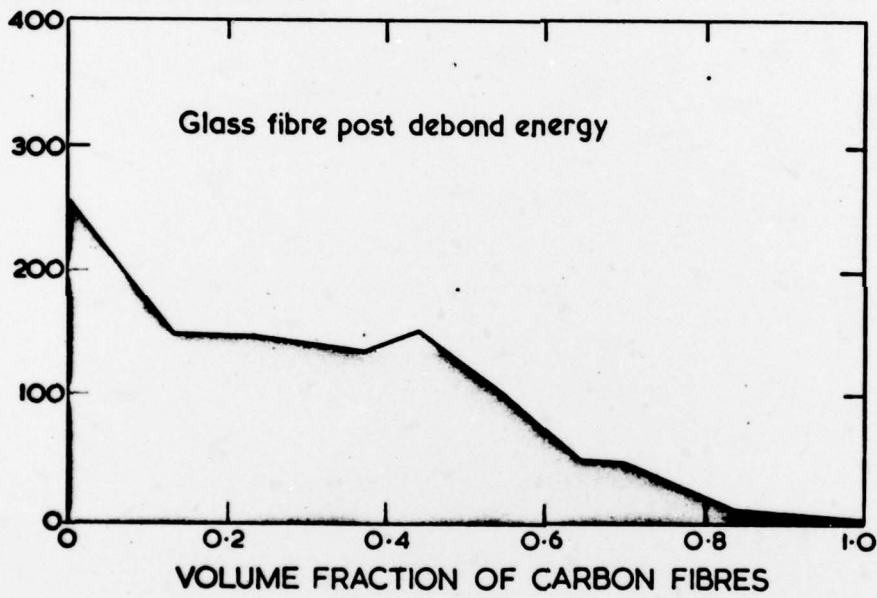
CUMULATIVE PROBABILITY



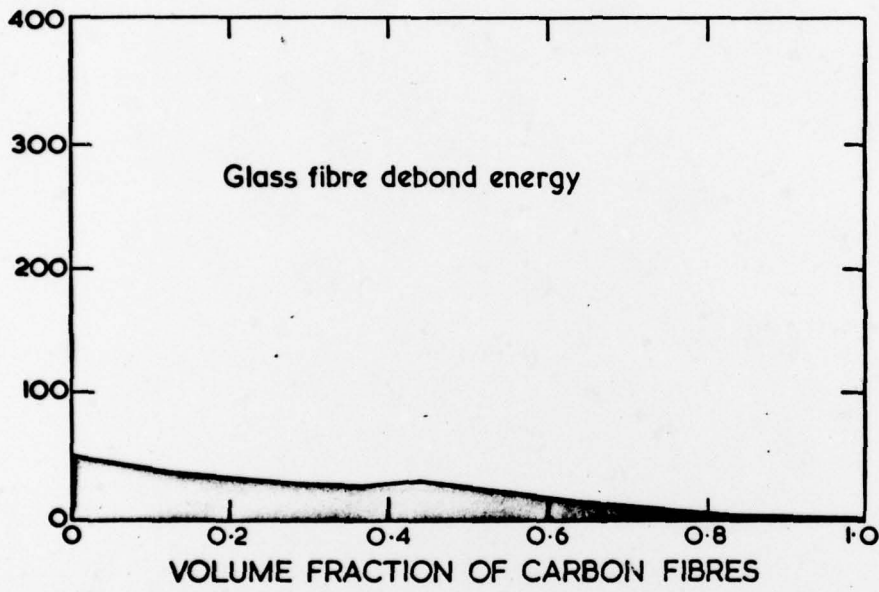
T_p (mm)

CARBON FIBRES

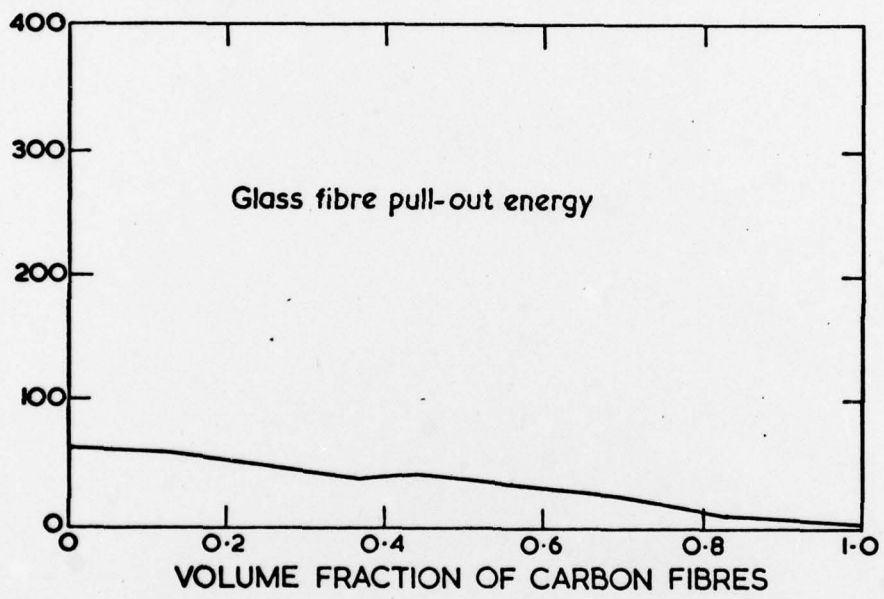
FRACTURE ENERGY (kJ/m²)



FRACTURE ENERGY (kJ/m²)



FRACTURE ENERGY (kJ/m²)



FRACTURE ENERGY (kJ/m²)

